Reaction Mechanism in Some O^{16} + $^{51}V^{51}$ Systems – A Comparative Study Using Numerical Integration Method and Computer Codes

Mohammed Abdella Siraj, A S Pradeep

Nuclear reaction mechanism in the energy range from 56MeV- 95MeV of some O^{16} + V^{51} systems have been studied. Excitation functions of various reaction products populated via Complete fusion and/or Incomplete Fusion of O^{16} projectile with V^{51} target were investigated at various projectile energies. The contributions of pre-equilibrium effect have been also examined. The theoretical values calculated using computer codes COMPLET, PACE4 have been compared with the experimental excitation functions data taken from EXFOR library. In addition to this a numerical integration method using MATLAB programming has been used to compare the experimental Excitation functions. A systematic study has been done by varying different parameters to see the effects on excitation function. The fair agreement of lower boundary energy for the reaction to occur with the experimental value has been shown by using MATLAB programming. The experimentally obtained reaction cross sections for non-α emitting channels were found to be in good agreement with theoretical predictions which may be attributed to complete fusion process at these energies, in general. However, for α- emitting channels, the experimental excitation functions exhibit a significant enhancement over the theoretical cross sections in the production cross section. The numerical approximation results depict enhancement in experimental ExcitationFunctions in an incomplete fusion reaction and is in good agreement in complete fusion and pre-equilibrium reaction mechanisms. An attempt has been done to estimate the percentage of incomplete fusion fraction to get the relative importance of complete and incomplete fusion reactions.

Index Terms—Cross Section, complete fusion, incomplete fusion, Excitation Functions, Level Density Parameter, Wong's formula and Numerical Integration Method

u

1 INTRODUCTION

Since the first nuclear reaction was observed almost a century ago [1], study of nuclear reactions leads to several fundamental discoveries, such as discovery of neutron, nuclear fission, production of a wide range of chemical elements up to the super heavy nuclei, production of sub-nuclear (elementary) particles, and production of a new state of matter, quark-gluon plasma. Moreover, a practical use of nuclear reactions influenced the daily life of human society through a wide range of applications, most prominently in production of energy and in medicine. Specific role belongs to the nuclear reactions, induced by the beams of heavy ions on heavy target nuclei.

Among the mechanisms of nuclear reactions processes, heavy ion reaction is one. For many years the study of heavy ion induced reaction has been used as important tool to understand the reaction dynamics and the decay characteristics of excited compound nuclei at energies near and above the coulombs barrier (CB) [2], [3]. In recent years, it has been observed that for low Z-projectiles (Z ≤ 10), like ^{12}C, ^{16}O and ^{20}Ne, with incident energies slightly above the coulomb barrier, interacting with medium and heavy mass targets, both the CF and ICF processes may be considered as the dominant reaction mechanism [2], [3].

· *Mohammed Abdella Siraj is currently teaching in Hawassa university in physics department, Ethiopia, PH-+251941863519.*
E-mail: Zerituamede6062@gmail.com
· *A S Pradeep (Co-Author name) is currentlAPIIIT, R K Valley, Idupulapaya, KadapaAndhra Pradesh, Pin 516330, India, PH-+917032736826*
E-mail: draspradeep@gmail.com

In recent years, the investigation of breakup effects on fusion reactions in heavy-ion collisions around the Coulomb barrier has been a subject of intense experimental and theoretical interests [4]. Various processes can take place after the projectile breaks up. One is the incomplete fusion (ICF) in which part of the fragments is absorbed by the target. When all the fragments fuse with the target, the process is called sequential complete fusion (SCF). The residues from ICF cannot be distinguished from those from CF, and hence only the Total Fusion cross section can be measured. In the heavy ion reaction systems, the decay of the excited compound nucleus through the emission of charged particles can be negligible and the separate measurements of the CF cross section can be achieved.

Pre-equilibrium reaction has been also observed contributing in the heavy ion reaction at energies just above the Coulomb barrier. Pre-equilibrium reaction [5] is neither direct nor compound nucleus reaction. In this types of reactions particles are emitted after the first stage of a nuclear interaction (direct reaction) but long before the attainment of statistical equilibrium (compound nucleus formation). Their time scale is intermediate between the very fast direct reactions and the relatively slow compound nucleus formation.

For the last four decades, the barrier penetration model developed by C. Y. Wong [6] has been widely used to describe the fusion reactions at energies not too much above the barrier and at higher energies, which obviously explains the experimental results properly. There are several codes which are used for theoretical calculations of cross section like ALICE91, CASCADE, PACE4, COMPLET etc. These codes calculate the EFs of light and heavy-ion induced reactions. The configura-

tions of these codes predict the total cross section only for the population of the residual nuclei. At moderate excitation energies, reactions induced by heavy-ion are found to proceed through compound nucleus as well as pre-equilibrium emission. As a result, precise measurement of EFs for such cases and their analysis may be used to find out the relative contribution of equilibrium and PE processes. With a view to provide a large set of cross section data and to study the mechanism of PE emission a program of cross section precise measurements and analysis of cross section for heavy-ion induced reaction is necessary. Moreover, a detail study that compares the measured cross section with that of calculated values in the energy range of 56MeV to 95MeV has not been done by triangulation of experimental data, computer code and MATLAB code. The purpose of this paper is to fill this gap by using a heavy ion induced reaction that uses a heavy ion projectile O^{16} on a medium mass target of V^{51} at various projectile energies ranging from 56 to 95Mev. Moreover, the study can be used as a base line for further investigations on heavy ion reaction using MATLAB and it can also be used in validating the results of PACE 4 and COMPLET computer codes.

In the present work, measured CSs for eight reactions $V^{51}(O^{16},1a2n)Cu^{61}$, $V^{51}(O^{16},4p2n)Co^{61}$, $V^{51}(O^{16},2a1n)Co^{58}$, $V^{51}(O^{16},2a3n)Co^{56}$, $V^{51}(O^{16},2a2p3n)Mn^{54}$, $V^{51}(O^{16},1p4n)Zn^{62}$, $V^{51}(O^{16},1p3n)Zn^{63}$ and $V^{51}(O^{16},2n)Ga^{65}$ in the incident energy range 56MeV- 95MeV were taken from literature [7],[8]. Reaction cross sections have been compared with theoretical predictions based on Numerical integrations with the MATLAB code, PACE4 and COMPLET codes. The nuclear level density parameter (LDP) is an important ingredient in the statistical model calculation of reaction cross section for both the codes PACE4 and COMPLET. The Complet code uses Exciton number and mean free path (MFP) multiplier as an important parameter in the pre-equilibrium model calculation.

2 COMPUTER CODES AND MATLAB FORMULATIONS

In the current study, an analysis of experimentally measured reaction cross section is made using numerical method and theoretical prediction of the PACE 4 and COMPLET codes. Reaction cross section relation is derived using Wong's formula with the help of the critical distance model and sharp cut of model. The derived formula for the reaction cross section is used to determine the lower boundary of the energy range used in this thesis.

A numerical method is employed on Wong's formula to approximate the reaction cross section for the heavy ion reaction $O^{16}+V^{51}$. A MATLAB code is written to find out the reaction cross section for the energy range from 56MeV-95MeV.

In addition to the numerical method, an analysis of experimentally measured reaction cross section is carried out using the theoretical prediction of the PACE 4 code and a COMPLET code. PACE4 code performs only the statistical equilibrium model calculations and doesn't take pre-equilibrium (PE) and in-complete fusion processes into consideration where as COMPLET code does not taken into account the possibility of in-complete fusion but it can compute fusion cross-sections and pre equilibrium cross sections.

2.1 Mathematical Methods for the Reaction Cross Section

The cross section in the fusion process can be written as the sum of partial cross sections

$$s_F = \frac{p}{K^2}\sum (2l+1)T_l F_l \qquad (2.1)$$

F_l is fusion probability for the l^{th} partial wave. And it represents for any reaction that contributes to the reaction cross section.

T_l is transmission coefficient

For light projectiles at energies just above the coulomb barrier the fusion cross section is quite close to the total reaction cross section. For heavier projectile at higher incident energy, the fusion cross section falls below the reaction cross section due to the growing importance of direct and deep inelastic scattering which takes place at higher angular momentum or impact parameter.

In order to obtain a simple expression for the fusion probability one usually uses the Hill and Wheeler approximation [9]. In this approximation the effective potential near the barrier radius is approximated by a parabola. So that the transmission probability is written as

$$T_l = \frac{1}{1+\exp[2f]} \qquad (2.2)$$

$$\text{where } f = \frac{p}{\hbar w_l}(V_l - E)$$

The above Hill–Wheeler expression is exact for a parabolic barrier and is approximated for potential barriers in heavy-ion collisions. The Hill–Wheeler approximation for fusion cross-section was further simplified by Wong using the following assumptions [6]

$$R_l = R_{l=0} = R$$
$$w_l = w_{l=0} = w$$

$$V_l(r) = V_B + \frac{\hbar^2}{2\mu r^2}\left(l + \frac{1}{2}\right)^2 \quad with \quad V_B = V_{l=0} \tag{2.3}$$

Thus, according to the Wong's approximation the fusion cross section can be written as

$$\sigma_F = \frac{\pi}{k^2}\sum_{l=0}^{\infty}(2l+1)\frac{1}{1+\exp\left(\frac{2\pi}{\hbar\omega}(V_l - E)\right)} \tag{2.4}$$

Since V_l can be written as

$$V_l = V_B + \frac{l(l+1)\hbar^2}{2\mu R_B^2}$$

$$= V_B + \frac{\hbar^2}{2\mu R_B^2}\left(l+\frac{1}{2}\right)^2 - \frac{\hbar^2}{8\mu R_B^2} \tag{2.5}$$

We may write the fusion cross section as

$$\sigma_F = W\left[\frac{1}{1+\exp\left[\frac{2\pi}{\hbar\omega}\left(V_B - \frac{\hbar^2}{8\mu R_B^2} - E\right)\right]\exp\left[\frac{2\pi}{\hbar\omega}\frac{\left(l+\frac{1}{2}\right)^2\hbar^2}{2\mu R_B^2}\right]}\right] \tag{2.6}$$

Where $W = \frac{\pi}{k^2}\sum_{l=0}^{\infty}(2l+1)$

For simplicity, let us replace the constants in the above equation with *m* and *a*:

$$m = \exp\left[\frac{2\pi}{\hbar\omega}\left(V_B - \frac{\hbar^2}{8\mu R_B^2} - E\right)\right] \quad and \quad a = \frac{2\pi}{\hbar\omega}\frac{\hbar^2}{2\mu R_B^2}$$

So that

$$\sigma_F = \frac{\pi}{k^2}\sum_{l=0}^{\infty}\frac{2(l+\frac{1}{2})}{1+m\exp(a[l+\frac{1}{2}]^2)} \tag{2.7}$$

As large number of the partial waves contribute to the fusion cross-section, the summation over l may be changed into the integration.

$$\sigma_F = \frac{\pi}{k^2}\int_{l=0}^{\infty}\frac{2(l+\frac{1}{2})dl}{(1+m\exp(a[l+\frac{1}{2}])^2)} \tag{2.8}$$

In order to evaluate the integral, let us change the variable of the integration from l to *x* by

$$x = \left(l+\frac{1}{2}\right)^2 \Rightarrow dx = 2\left(l+\frac{1}{2}\right)dl$$

So that Eq. 2.8 becomes

$$\sigma_F = \frac{\pi}{k^2}\int_{l=1/4}^{\infty}\frac{dx}{[1+m\exp(ax)]} \tag{2.9}$$

$$\sigma_F = \frac{\pi}{k^2}\int_{l=1/4}^{\infty}\frac{\exp(-ax)dx}{[\exp(-ax)+m]} \tag{2.10}$$

Now again let $u = \exp(-ax) \Rightarrow du = -\frac{1}{a}\exp(-ax)dx$

$$\Rightarrow \exp(-ax) = -adu$$

$$\sigma_F = \frac{\pi}{k^2}\int_{\exp(-\frac{a}{4})}^{0}-\frac{du}{a(m+u)} \tag{2.11}$$

The integration with respect to u results

$$\sigma_F = \frac{\pi}{ak^2}ln[m+u]_{\exp(-a/4)}^{0} \tag{2.12}$$

$$= \frac{\pi}{ak^2}\left(ln[m+\exp(-a/4)] - ln[m]\right)$$

$$= \frac{\pi}{ak^2}ln\left[1+\frac{\exp(-a/4)}{m}\right]$$

By putting the values of $k = \sqrt{\frac{2\mu E}{\hbar^2}}$, *m* and *a*, we get the following final expression of Wong's formula for the reaction cross-section

$$\sigma = \frac{\hbar\omega R_B^2}{2E}ln\left[1+\exp\left(\frac{2\pi}{\hbar\omega}(E - V_B)\right)\right] \tag{2.13}$$

where $\hbar\omega$ is the curvature of the inverted parabola.
For a relatively large value of E, the above result reduces to a well-known formula

$$\sigma_R = \pi R_B^2\left(1 - \frac{V_l(R_B)}{E_{cm}}\right) \tag{2.14}$$

For relatively small value of E, such that $E << V_B$

$$\sigma = \frac{\hbar\omega R_B^2}{2E}\exp\left[2\pi\left(\frac{1}{\hbar\omega}(E - V_B)\right)\right] \tag{2.15}$$

The Critical Model [10] assumes that fusion takes place whenever the trajectory is such that at some stage the projectile and the target mass centers are separated by a 'critical' distance R_c which is somewhat smaller than the position of the barrier R_B.

At this distance the attraction nuclear force are supposed to be sufficiently strong to pull the projectile and target together.

At the critical distance

$$\sigma_R = \pi R_C^2 \left(\frac{E_{cm} - V_l(R_C)}{E_{cm}}\right) = \pi R_C^2 \left(1 - \frac{V_B(R_C)}{E_{cm}}\right) \quad (2.16)$$

Where R_c is the critical distance given by

$$R_C = 1.0\left(A_P^{1/3} + A_T^{1/3}\right) fm$$

A_p *and* A_T are the atomic mass of the projectile and

target respectively?

The barrier potential is

$$V(R_c) = \frac{Z_P Z_T e^2}{R_c} \quad (2.17)$$

The center of mass energyis

$$E_{cm} = E_{lab}\left(\frac{A_T}{A_T + A_P}\right) \quad (2.18)$$

The present work falls under the category of heavy- ion (^{16}O) induced reaction on a middle mass target (^{51}V). Using the critical distance model discussed above, the reaction cross section can be approximated for the reaction $^{16}O + ^{51}V$ as

$$\sigma_R = \pi R_C^2 \left(1 - \frac{V(R_C)}{E_{cm}}\right)$$

$$\sigma_R = R x \left(1 - \frac{Z_O Z_V (1.6x10^{-19})^2 c^2}{1.0\left(A_O^{1/3} + A_V^{1/3}\right) fm \left(E_{lab}\left[\frac{A_V}{A_V + A_O}\right]\right)}\right) \quad (2.19)$$

Where $fm = 10^{-15} m$, and

$$R = \pi\left(1.0\left[A_O^{1/3} + A_V^{1/3}\right]\right)^2 (fm)^2$$

A_o =atomic mass of oxygen, A_V=atomic mass of Vanadium, Z_o=atomic number of oxygen and

Z_T =atomic number of Vanadium

From the above equation we can understand that the reaction cross section depends on the atomic mass, atomic numbers of both the projectile and the target and the bombarding energy (E_{lab}).

Using the known values in equation 2.19, the reaction cross section becomes

$$\sigma_R = q\, x \left(1 - \frac{[1.44Mev] Z_O Z_V}{\left(\left[\frac{A_V}{A_V + A_O}\right][A_V^{1/3} + A_O^{1/3}]\right) E_{lab}}\right) \quad (2.20)$$

$$where \qquad q = (31.4mbarn)\left(\left[A_O^{1/3} + A_V^{1/3}\right]\right)^2$$

For any heavy ion reaction of type $T(p,x)Y$, the reaction cross section can be written as:

$$\sigma_R = n\, x \left(1 - \frac{[1.44Mev] Z_p Z_T}{\left(\left[\frac{A_T}{A_p + A_T}\right][A_p^{1/3} + A_T^{1/3}]\right) E_{lab}}\right) \quad (2.21)$$

$$where \quad n = (31.4mbarn)\left(\left[A_p^{1/3} + A_T^{1/3}\right]\right)^2$$

Using the appropriate values of atomic mass and atomic number for the reaction $V^{51}(O^{16}, x)Y$, the reaction cross section will be reduced to

$$\sigma_R(mb) = 1.22\left(1 - \frac{56Mev}{E_{lab}}\right) \quad (2.22)$$

From the above equation, we can determine the minimum projectile energy that results the lowest reaction cross section by letting $\sigma_R = 0$.

$$\sigma_R = 1.22 - \frac{68.2Mev}{E_{lab}} = 0$$

$$\therefore E_{lab} = \frac{68.2Mev}{1.22} = 56Mev.$$

Alternatively, we can estimate this minimum energy from the projectile energy Vs cross section graph as shown in Fig 2.1 plotted using a MATLAB script:

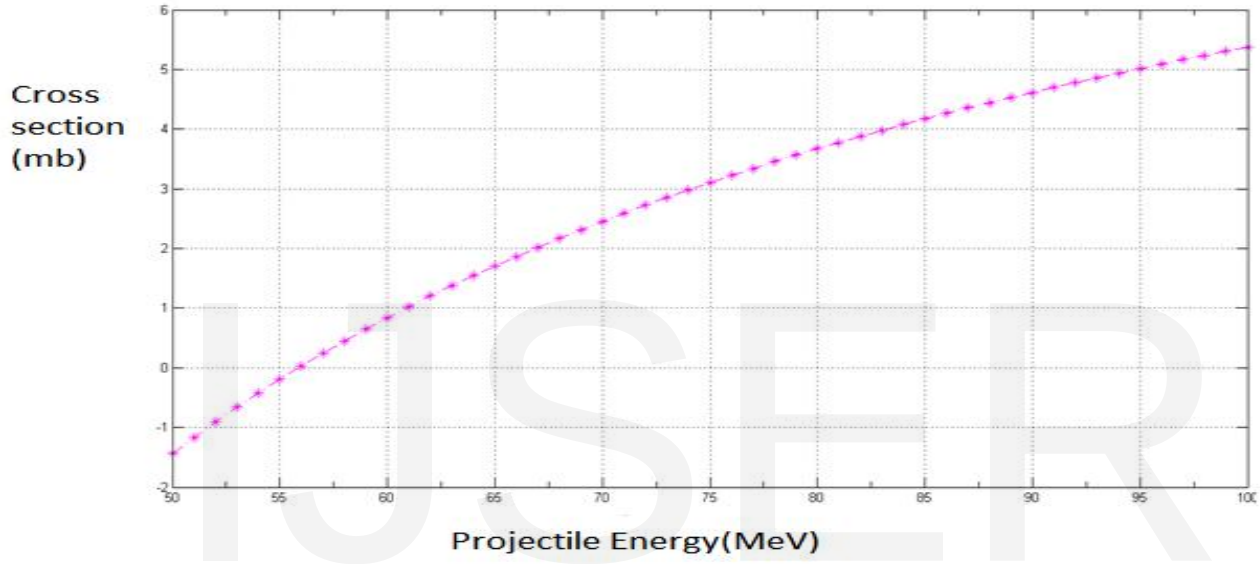

Fig. 2.1 projectile energy-cross section for the reaction O^{16} + V^{51} using MATLAB code

From the graph it can be inferred that the cross section becomes zero when the projectile energy is approximately 56Mev. The calculated value is in good agreement with the lowest energy used in the experimental data taken from EXFOR which is 58MeV.

Therefor the reaction cross section can be calculated with laboratory energy greater than 56MeV in all the theoretical calculations for the current paper.

2.1.1 Numerical Integration

The exact solution for reaction cross section in equation 2.11 and 2.14 is reached as the result of integration by the change of variable method. In this part, the reaction cross section formula will be approximated numerically using the numerical integration techniques of Simpson's 1/3 rule taking equation 3.11.

The general relation to approximate the integration of a function *f* using Simpson's one-third rule can be derived as [11]

$$\int_{x_0}^{x_n} f(x)dx \approx \frac{x_n - x_0}{3n}\left[f(x_0) + 4\sum_{i=1,3,5}^{n-1} f(x_i) + 2\sum_{i=2,4,6}^{n-2} f(x_i) + f(x_n)\right] \quad (2.24)$$

for Simpson's one-third rule where n is the number of segments in between x_0 *and* x_n,

The error estimate for Simpson's one third rule if *f(x)* is four times differentiable in the interval $[x_0, x_n]$ and that $|f^4(x) \le M|$ for some finite *M*. Hence the maximum error allowed will be $e = \frac{M(x_n - x_0)^5}{180n^4}$

Using this error estimation, the number of segments in between x_0 *and* x_n can be determined for the appropriate value of x_0 *and* x_n as shown in equation 2.27 below.

From equation 2.11 we have

$$s_F = \frac{p}{k^2} \int_{\exp(-\frac{a}{4})}^{0} - \frac{du}{a(m+u)} \quad ,$$

$$f(x) = f(u) = - \frac{1}{a(m+u)}$$

Where $k = \sqrt{\frac{2m}{\hbar^2}E}$,

$m = \exp\left(\frac{2p}{\hbar w}\left[V_B - \frac{\hbar^2}{8mR_B^2} - E\right]\right)$ and

$$a = \frac{2p}{\hbar w}\frac{\hbar^2}{2mR_B^2}$$

To determine the value of m and a, the value of curvature of the coulomb barrier $\hbar w$ has to be known.

To obtain the curvature of the coulomb based on the Wood's Saxon potential, the region around the top of the CB can be approximated by an inverted harmonic oscillator potential of height V_B and frequency w.[12]

$$\hbar w = \hbar\sqrt{\frac{Z_P Z_T e^2}{mrR^2{}_B}\left(1 - \frac{2r}{R_B}\right)} \qquad (2.25)$$

Where r *is surface diffusivity*

For near spherical nuclei small diffusivity 0.6 can describe fusion data [13].

For the reaction $O^{16} + V^{51}$ applying Taylor expansion on equation 2.25,

$$\hbar w = \frac{A}{\sqrt{r}} - B\sqrt{r} \qquad A = \frac{\hbar}{R_B}\sqrt{\frac{Z_P Z_T e^2}{m}}$$

$$and \;\; B = \frac{\hbar}{R_B^2}\sqrt{\frac{Z_T Z_P e^2}{m}} \qquad (2.26)$$

$$A = \sqrt{\frac{8x23x(1.6x10^{-19}c)^2 x9x10^9 \frac{N - m^2}{C^2}}{\frac{16x51x1.66x10^{-27}}{67}}}$$

$$= \frac{6.58x10^{-22}}{6.23}\sqrt{2.19} = 1.53x10^{-7}$$

$$B = \frac{6.58x10^{-22}}{(6.23\,fm)^2}x\sqrt{2.19} = 0.245x10^8$$

$$\hbar w = \frac{A}{\sqrt{a}} - B\sqrt{a} = \frac{1.53x10^{--7}}{\sqrt{r}} - 0.24510^8\sqrt{r} \;,$$

for surface diffusivity $r = 0.63\,fm$

$$\hbar w = \frac{A}{\sqrt{a}} - B\sqrt{a} = \frac{1.53x10^{--7}}{\sqrt{0.63\,fm}} - 0.24510^8\sqrt{0.63\,fm}$$

$$= 6.95 - 0.539 = 6.41MeV$$

Hence

$$a = \frac{2p}{\hbar w}\frac{\hbar^2}{2mR_B^2} = \frac{6.28}{6.41}\frac{(6.58x10^{-22})^2 x1.6x10^{-13}}{2x12.2x1.66x10^{-27}(6.23x10^{-15})^2}$$

$$= \frac{435}{10077} = 0.0432$$

$$m = \exp\left(\frac{2p}{\hbar w}\left[V_B - \frac{\hbar^2}{8mR_B^2} - E\right]\right)$$

$$= \exp\left(\frac{6.28}{6.41}\left[V_B - \frac{(6.58x10^{-22})^2}{8x12.2x(6.23x10^{-15})^2} - E\right]\right)$$

$$m = \exp\left(0.98\left[V_B - 1.14\,x10^{-16} - E\right]\right)$$

$$\Rightarrow \; m \approx \exp\left(0.98\left[56 - E\right]\right)$$

Using the values of m and a, the cross section can be put as

$$s_F = \frac{p}{k^2}\int_{\exp(-\frac{a}{4})}^{0} - \frac{du}{a(m+u)} = \left(\frac{p\hbar^2}{2mE}x\frac{\hbar w 2mR^2}{2p\hbar^2} = \frac{\hbar wR^2}{2E}\right)\int_{0.989}^{0} - \frac{du}{m+u}$$

$$s_F = \frac{\hbar wR^2}{2E}\int_{0.989}^{0} - \frac{du}{m+u} \qquad (2.27)$$

2.2 The MATLAB code

The numerical approximation can be determined using different numerical integration techniques [11]. Among the techniques are the trapezoidal rule, Simpson's one third rule and Simpson's three-eight rules. The function that helps us to calculate the reaction cross section was first formulated in section 2.1 as equation 2.27. Using this equation, a MATLAB code was developed using Simpson's one third rule that approximates

the integration of the function numerically as shown in equation 2.26. The MATLAB code calculates the reaction cross section when the specific projectile energy value is used after it evaluated the value for the function indicated in equation 2.27. Using the upper and lower limits in equation 2.27, the number of segments necessary to calculate the approximation is determined using the error estimation equation.

$$e = \frac{M\,(x_n - x_0)^5}{180\,n^4}$$

3. RESULTS AND DISCUSSION

,

The CSs of eight residue nuclei have been compared and analyzed with theoretical predictions based on Numerical Approximation using MATLAB code, PACE4 and COMPLET codes. The lower boundary projectile energy was taken from the reults of calculations using equation 2.17. In the current study, to compare the theoretical cross section with the experimental data the excitation functions will be calculated by a reasonable combination of the level density parameter k, initial excitation number n, and MFP multiplier. To this end, effect of parameter varation is employed.

3.1 Effects of Parameter Variations on the Theoretical Calculations

The best combinations of the parameters used in this paper are detrmined so that uniform values of these parameters will be used in calculating the EFs for the production of the eight residue nuclei. Theoretical cross section compared with experimental data by varying level density parameters for randomly choosen $V^{51}(O^{16},1p3n)Zn^{63}$ reaction.

PACE4 CODE

The important parameter in the PACE4 code is the level density parameter ‘a’. The level density parameter ‘a’ is calculated using the relation a=A/k, where A is the mass number of the compound system and k is a free constant which may be varied to match the experimental data. Hence to determine the value of k for the best fit data the free constant k is varied from 8 to 10 by step one for $V^{51}(O^{16},1p3n)Zn^{63}$ reaction.

COMPLET CODE

The parameters that play important role in the calculations of excitation function are the level density parameter ‘a’ for the compound nucleus formation and the exciton number n and the mean free path multiplier *MFP for the pre-compound formation.* These parameters were used in this code to observe the varation effect.

Table 3.1- Experimentally measured cross sections (in mb) for the eight residues Nuclei

E_{LAB}(MEV)	Residue Nuclei							
	Cu^{61}	Co^{61}	Co^{58}	Co^{56}	Mn^{54}	Zn^{62}	Zn^{63}	Ga^{65}
58.1	-	-	-	-	-	-	-	7.7
58.3	-	-	-	-	-	-	28	-
58.4	-	13.3	-	-	-	-	-	-
60	213.6	-	46.8	-	23.5	0.5	-	-
68.9	-	-					78	
69	267	-	88.3	-	42.3	1.9	-	-
69.4	-	17.1	-	-	-	-	-	-
69.6	-	-	-	-	-	-	-	1.18
71.7	-	20.6	-	-	-	-	-	-
72.1	-	-	-	-	-	-	94	-
72.2	-	-	-	-	-	-	-	0.46
79.8	204.9	-	106.1	2.16	80.9	14.6	-	-
82.1	-	-	-	-	-	-	109	-
82.2	-	-	-	2.4	-	-	-	-
82.3	-	23	-	-	-	-	-	-
87.4	-	-	-	12.5	-	-	37	-
92	94.3	-	73.2	15.25	108	28.1	-	-
93.3	-	-	-	-	-	-	32	-
93.4	-	14.1	-	-	-	-	-	-
93.5	-	-	-	23	-	-	-	-

Source: International Atomic Energy Agency (IAEA)-Nuclear Data Services, Experimental Nuclear Reaction Data (EXFOR), Vienna, Australia,

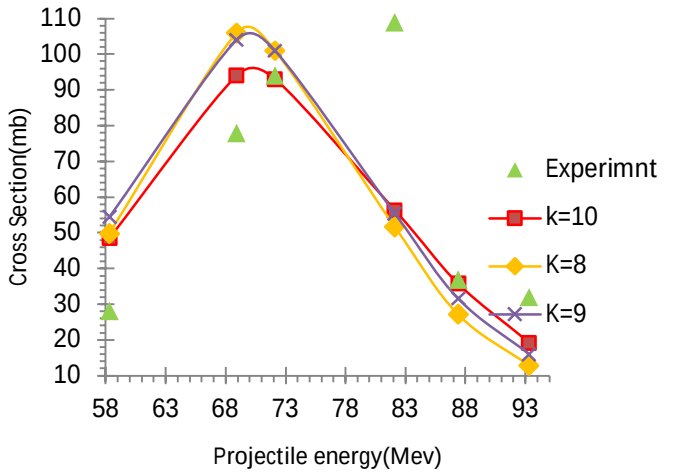

Fig. 3.1.1 Theoretical cross section compared with experimental data by varying level density parameters

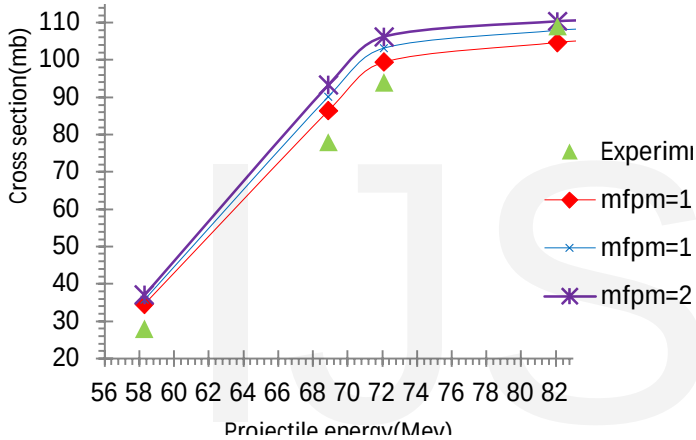

Fig. 3.1.2 Theoretical cross section compared with experimental data by varying mean free path multiplier

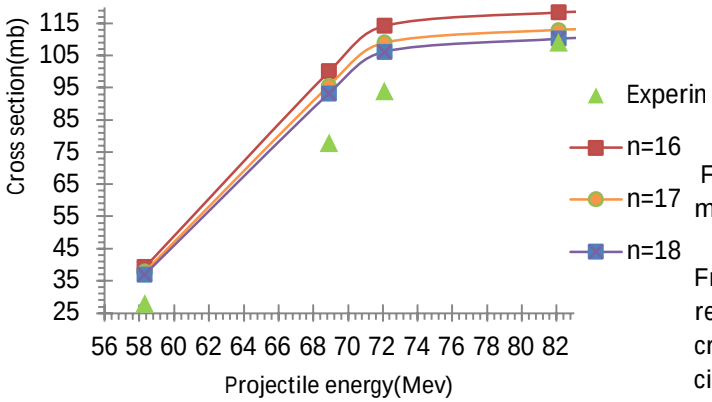

Fig. 3.1.3 Theoretical cross section compared with experim ental data by varying exciton number

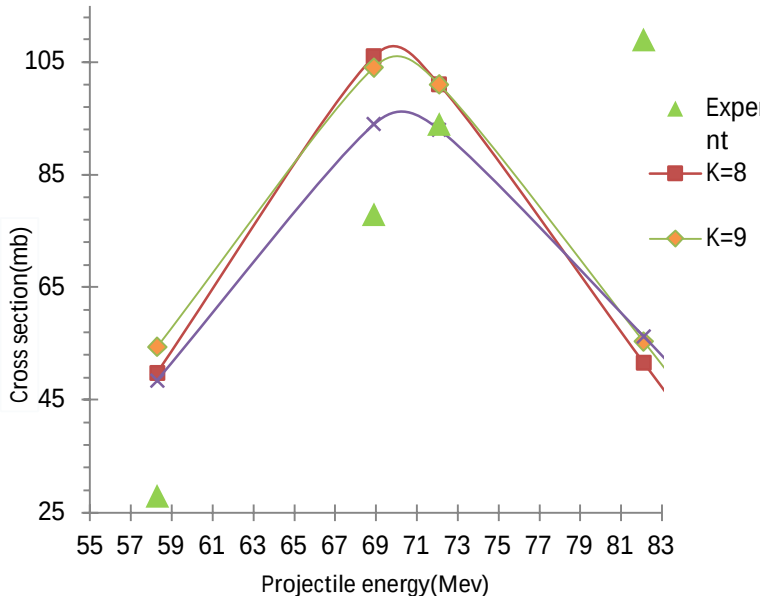

Fig. 3.1.4 Theoretical cross section compared with experimental data by varying level density parameter

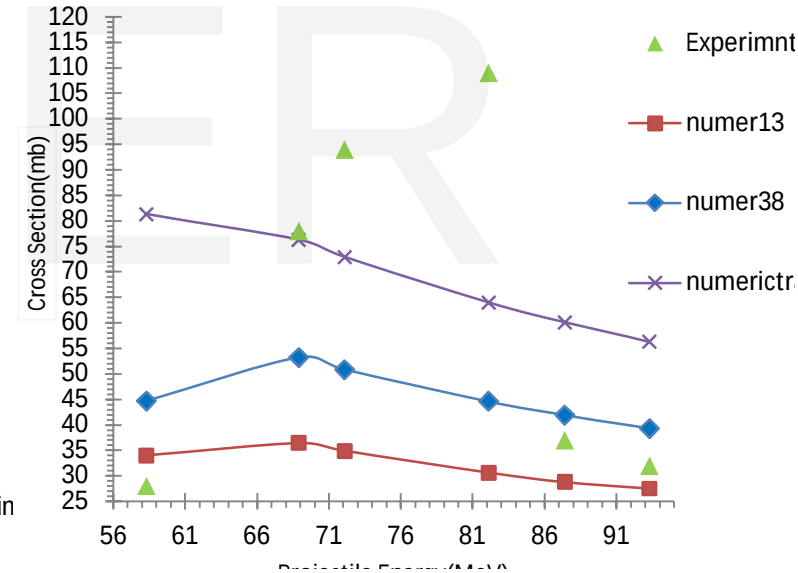

Fig. 3.1.5 Theoretical cross section compared with experimental data by changing the numerical method

From figures 3.1.2 and 3.1.3, it can be observed that the theoretical prediction is fairly comparable with the experimental cross section for the mean free path multiplier *MFP*=1 and exciton number n=18.The variation in level density parameter shows a slight agreement between the theoretical and experimental cross section as shown in figure 3.1.4 for k=10. Hence level density parameter k=10 might be preferably chosen compared to the remaining level density parameters.

Accordingly, from the results of graphs 3.1.1-3.1.4, the best combination of parameters for the analysis and calculations of

excitation function will be level density parameter k=10 for PACE4 code and mean free path multiplier MFP=1, exciton number n=18 and level density parameter k=10 for COMPLET code.

The effects of the variation of numerical approximation technique on reaction cross section was also made and for higher and lower extreme of projectile energy in figure 3.1.5, the numerical methods agree with the experimental data. At those agreements, Simpson's one third method is comparably better than both the Simpson's 3/8 rule and trapezoidal rule.

Based on this combination, the theoretical cross section will be compared and analyzed for the residue nuclei Cu^{61}, Co^{61}, Co^{58}, Co^{56}, Mn^{54}, Zn^{62}, Zn^{63} and Ga^{65} below.

3.2 Excitation Functions for Experimentally Measured and Theoretically Calculated Values

In the production of residue nucleus Cu^{61}, experimentally measured cross section is higher than the theoretically calculated values for PACE4 C and the numerically obtained data as shown in the figure 3.2.1. The enhancement in the measured value over theoretical value can be attributed to ICF's dominant reaction mechanism in which the break-up of ^{16}O in to $^{14}C + a_2^4$ may occur at higher energies. The fragment ^{14}C completely fuses with the target forming an excited CN of Zn^{65*} and leaving a_2^4 as a spectator. The compound nucleus emits two neutrons while it de-excites. The enhancement in the experimental cross section is more for PACE4 at higher energies. The numerical data calculated using MATLB displays the disparity between the calculated and measured data in agreement with the theoretical predictions of PACE4 and especially it fits with the PACE4 for higher energies. The COMPLET code only agrees with the PACE4 predictions only for 69Mev

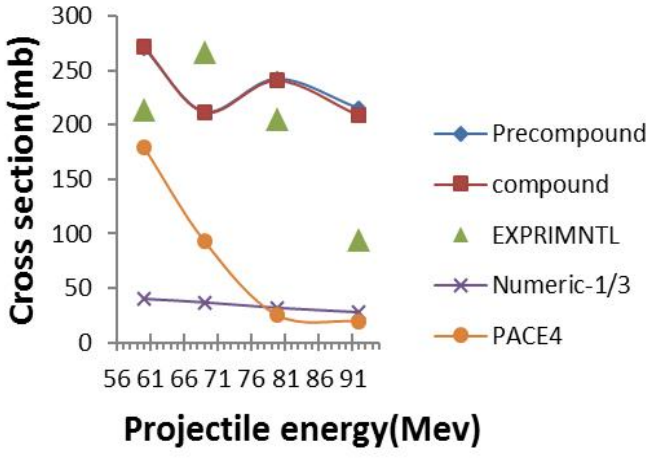

Fig.3.2. 1 Production of Cu^{61}

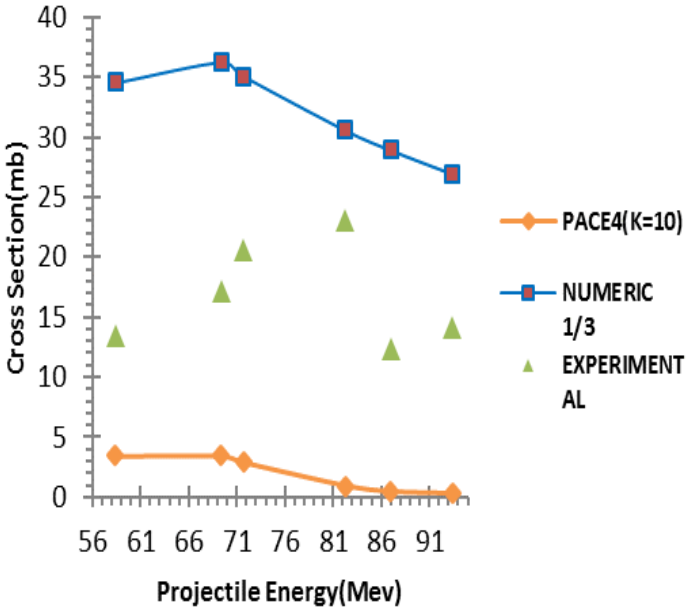

Fig. 3.2.2 Production of Co^{61}

It can be clearly observed that the experimental data is much higher than the calculated data in the production of the evaporation residues ^{61}Co. Hence the theoretical value obtained using PACE4 Code could not reproduce the experimental data indicating the contribution from incomplete fusion reactions of the projectile with the target.

There may be a breakup of ^{16}O into ^{12}C and a_2^4 with subsequent incomplete fusion of ^{12}C in the reaction ^{51}V (^{16}O, A) ^{63}Cu; the evaporation of two protons leads to the formation of the residues. The results of the numerical integration are above the experimental data. Hence it is unable to identify the ICF contributions in the production of ^{61}Co.

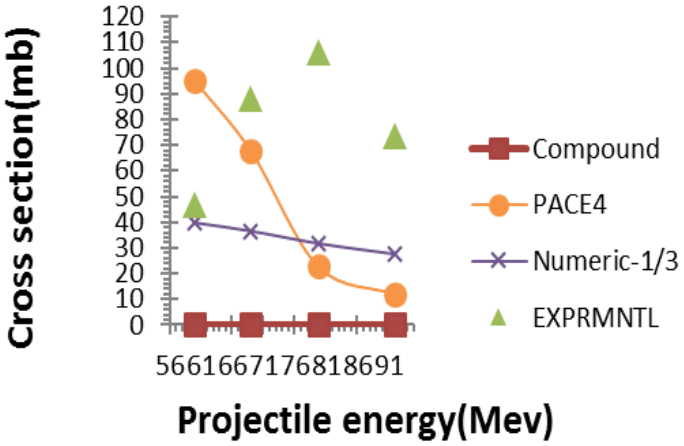

Fig. 3.2.3 Production of Co^{58}

.

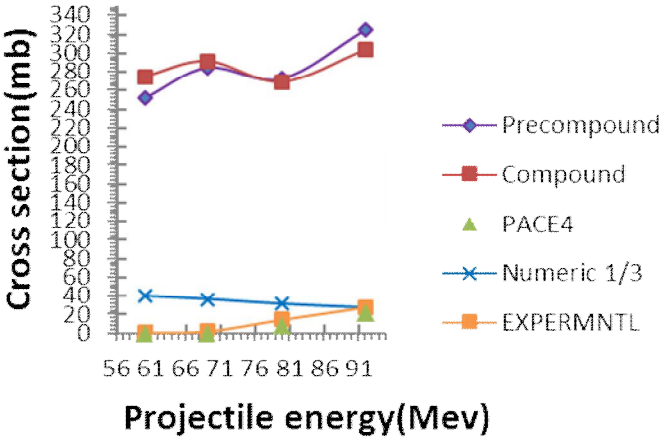

Fig. 3.2.6 Production of Zn^{62}

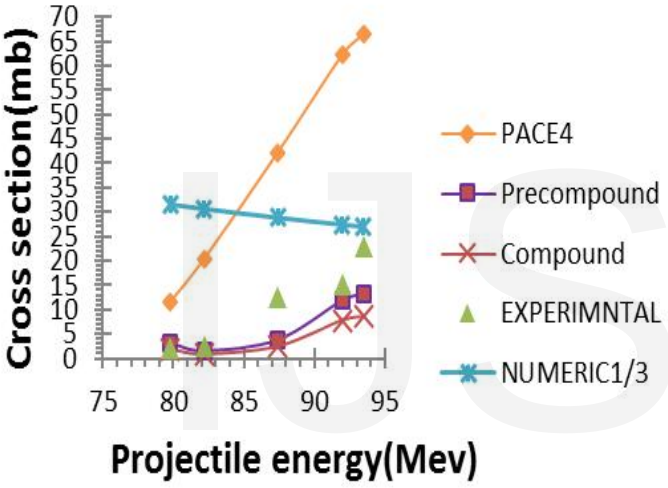

Fig. 3.2.4 production of Co^{56}

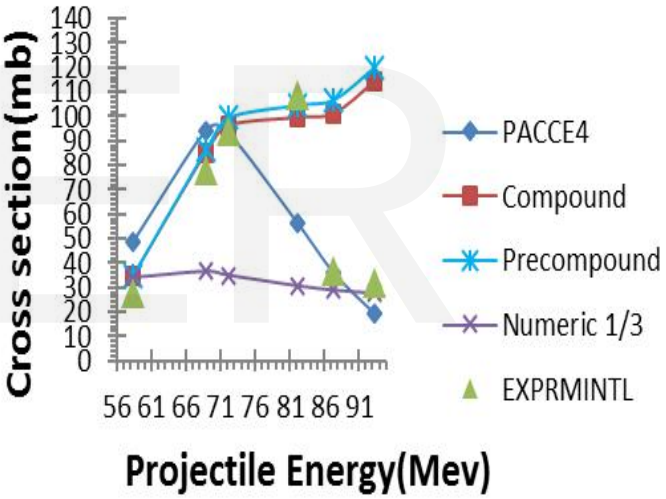

Fig. 3.2.7 Production of Zn^{63}

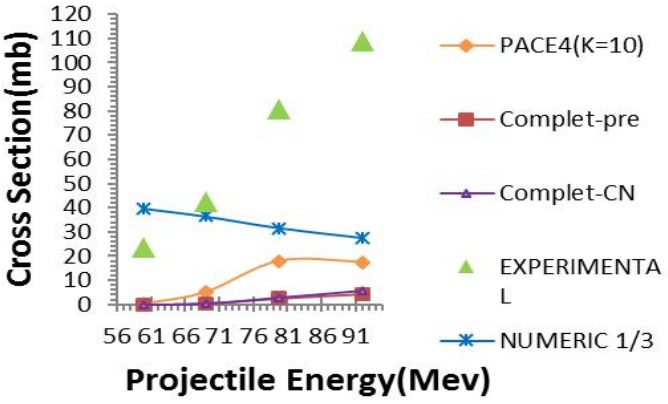

Fig. 3.2.5 Production of Mn^{54}

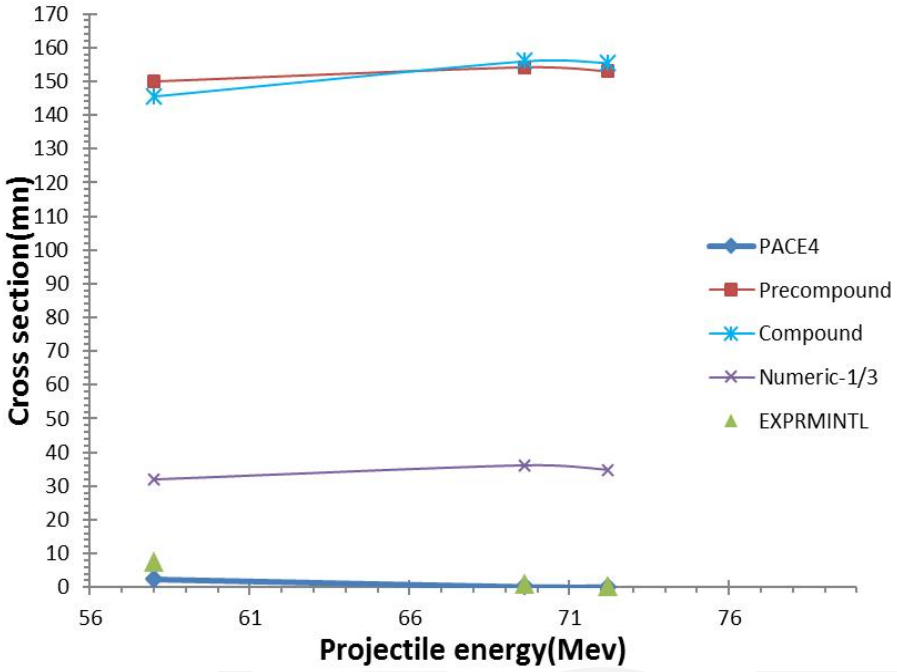

Fig. 3.2.8 Production of Ga^{65}

From figure 3.2.3, it can be seen that the experimental data were much and higher than the theoretical value of the two codes including the numerical approximation especially at projectile energy greater than 60MeV. There is a significant enhancement in the experimental cross section over the theoretical cross section. Hence for the production of Co^{58}, there is a dominant contribution from ICF reaction process. The projectile may break-up into $2a$ and ^{8}Be where ^{8}Be fuses with the target forming a CN and leaving $2a$ as a spectator. The excited CN Co^{59*} emits on neutron during its de-excitation.

The numerical data signifies the ICF contribution in agreement with the PACE4 and COMPLETE codes.

In the reaction $V^{51}(O^{16},2a3n)Co^{56}$, the experimental data is reproduced by calculated data obtained through the Complete Code for pre-equilibrium reaction for almost all the projectile energies as shown in figure 3.2.4. Hence a pre-equilibrium reaction has a significant contribution for this reaction. As the energy of the projectile increases, the experimental result is showing a slight rise compared to the theoretical values. This difference in the experimental and theoretical calculations may be attributed to errors made in both the experiment and the code.

The numerical data and the PACE4 result show agreement with the experimental values at higher and lower energies respectively. In the production of Mn^{54} the experimental data is very much higher than the `theoretical data calculated using PACE4 and COMPLET CODES. This enhancement of the measured values over the calculated ones is as a result of the contribution from the ICF reaction process. The excited CN formed from fusion of ^{8}Be with ^{51}V emits two protons and three neutrons subsequently during its de-excitation. The numerical approximation data calculated using MATLB displays this disparity between the calculated and measured values as shown in figure 3.2.5 at higher energy. In the reaction $V^{51}(O^{16},1p4n)Zn^{62}$ theoretically obtained, especial-

ly from PACE4, results are comparable to the experimentally measured data as shown in figure 5.2.6. So in this reaction the projectile O^{16} is assumed to be fuse completely with the target nucleus V^{51} forming the excited state Ga^{67*}, and this excited state emits four neutrons and one proton, during the thermalization, leaving behind the residual nucleus Zn^{62}.

The numerical data agrees with the PACE4 in reproducing the measured date especially at higher energies. In this reaction the projectile completely fuses with the target. The Complete code has a cross sectional data that does not agree with the measured values. In the production of $Zn^{63,}$ the experimental data is reproduced by calculated cross section using COMPLET code for the compound nucleus formation as shown from figure 3.2.7. Hence the projectile is completely fused with the target forming an excited nucleus that subsequently emits three neutrons and one proton during its de- excitation. The agreement implies the contribution of the CF is dominant for this reaction. The numerical calculation agrees to this outcome for the lower and higher energies as shown in the figure and the PACE4 data also supports the complete fusion reactions. In this reaction the excited nuclei Ga^{67*} emits two neutron forming a residue nucleus of Ga^{65}. The theoretically calculated cross section using PACE4 is perfectly matching with the experimental value for level density parameter K=10. Hence it can be said that the projectile is completely fused with the target indicating the contribution of CF reaction's dominance based on the PACE 4 code.

It can be observed from figure 3.2.6, 3.2.7 and 3.2.8 that the EFs for the production of Zn^{62}, Zn^{63} and Ga^{65} is in fair agreement with the theoretical predictions made by PACE4 code and COMPLETE code for compound nucleus formation. These evaporation residues are produced as a result of proton and neutron emission in *xn* and *pxn* channels of reaction without involving a emission. Hence it can be said that the *xn* and *pxn* channels are populated via the CF.

The evaporation residues produced by the reactions $V^{51}(O^{16},1a2n)Cu^{61}$, $V^{51}(O^{16},2a1n)Co^{58}$, $V^{51}(O^{16},a2p)Co^{61}$ and $V^{51}(O^{16},2a2p3n)Mn^{54}$ involve a -emissions. The theoretical values could not reproduce the experimental value as shown in the figure 3.2.1-3.2.4 and figure 3.2.6. As the PACE4 model predicts the cross section for CF only and COMPLET code predicts pre-equilibrium and compound nucleus formation, the difference in cross section between experimental and theoretical cross sections can be attributed to incomplete fusion reaction.

In the production of Co^{56}, a pre-equilibrium reaction mechanism was detected as the experimental data fits with the COMPLET code data for pre-equilibrium reactions.

3.3 Percentage Fraction of Incomplete Fusion

From the above discussions it is evident that the ICF reaction contributes significantly to the evaporation residue cross section. This contribution can be analyzed further using Gomes et al., [14] by determining the difference of the total measured cross section and total PACE4 reaction cross sections for all a -emitting channels.

Hence the % ICF fraction can be calculated as $\frac{\sum s_{ICF}}{\sum s_{TF}} x100$.

This percentage fraction against the projectile energy is plotted in figure 4.3.1. This figure shows that the total ICF cross section below the experimental cross section and more importantly it is increasing as projectile energy increases.

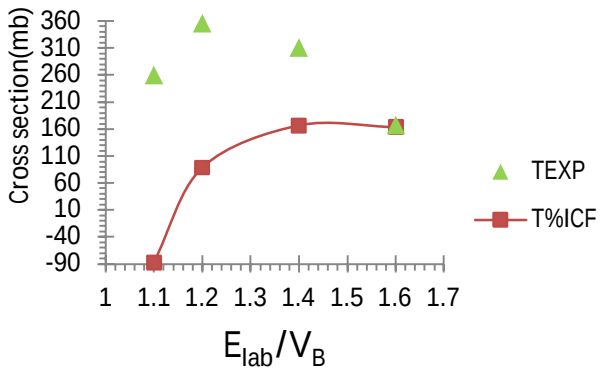

Fig.3.3.1 E_{lab}/V_B versus Percentage fraction of ICF for $a2n$ *and* $2an$ reactions

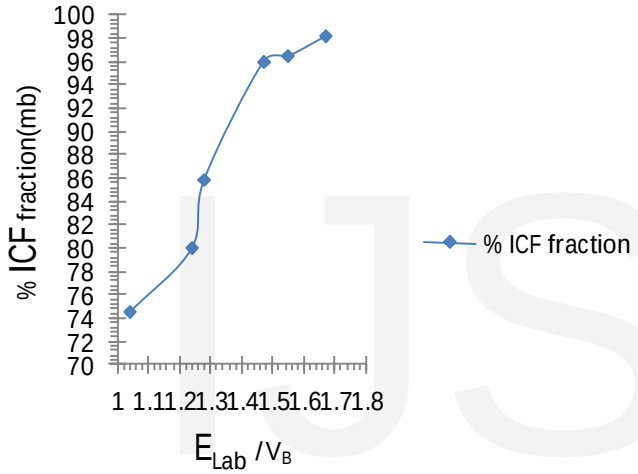

Fig. 3.3.2 E_{lab}/V_B versus Percentage fraction of ICF for $a2p$

4. CONCLUSION

In the present work the cross sections of eight evaporation residue were studied as a result of the heavy ion induced reaction of ^{16}O + ^{51}V in the energy range 56Mev-95Mev. The study can be used as a base line for further investigations of reaction cross section on heavy ion reaction using MATLAB. It can also validate the the outcomes of computer codes as it involves triangulation for the analysis of cross section data from experimental value, computer codes and MATLAB programing. Diffeent channels of reaction were observed namely: *xn, pxn, αxn, αxp, 2αxn and 2αxpxn* for *x* = 2,3 and 4. The reaction cross sections were calculated in three different ways using Numerical a proximation with MATLAB program, COMPLET code and PACE4 code. In these reactions, it can be concluded that the comparison of the calculated data with the experimental data showed the reaction mechanisms Pre-equilibrium reaction, the Complete Fusion (CF) and Incomplete Fusion (ICF) were involved in the production of the residue nuclei. In all a -emitting channel of reactions, the theoretical data could not reproduce the experimental data indicating negligible contributions from CF. Hence, it can be concluded that dominant contribution comes from the incomplete fusion that takes places as a result of break-up of the projectile ^{16}O in to a and C^{12} in the production of Cu^{61} and Co^{61}, and break -up of the projectile O^{16} in to $2a$ and Be^{8} in the production of Co^{58}, Mn^{54}. The non-a emitting channels of reactions in the production of Zn^{62}, Zn^{63} and Ga^{65} undergo complete fusion of the projectile O^{16} in to the target V^{51}. This is quite expected as this evaporation residue is associated with the emission of neutron and proton in *xn and pxn* channels of reaction without involving a emission. Hence it can be generally said that the xn *and pxn* channels are populated via the CF.

In the case of residue nucleus Co^{56} the dominant reaction comes from pre-equilibrium reaction mechanisms. This is an evidence for the contribution of pre-equilibrium reactions in heavy ion reaction.

The numerical data calculation was done using MATLAB program based on fusion cross section of Wong's formula. This data fairly agrees with predictions of PACE4 and COMPLET code results as in the a -emitting channels. It also agrees with the prediction of the two codes in reproducing the experimental data in the production of Zn^{62} and Zn^{63} which are non a -emitting channels.

As such, it may be concluded that apart from CF, the ICF is also a process of greater importance even at the low energies and hence, while predicting the total reaction cross-sections, ICF contribution should also be taken into consideration. Further, as expected percentage fractions for the α2n, $2an$ and $a2p$ channels of reactions is found to increase with increasing energy.

ACKNOWLEDGEMENTS

The authors wish to thank *prof. A K Chauby, Adiss Ababa University* for his relentless support, and Mr. Solomon Tekeste Asta for his financial support.

[1] M Veselsk, "Nuclear Reactions with heavy ion beams," Institute of Physics, *Slovak Academy of Sciences, 1*-2, 2013

[2] Ali S, Ahmad T, Kumar, K, Rizvi I.A, Agarwal A, Ghugre S.S, Sinha A.K, Chaubey," Effect of Projectile Break-Up Threshold Energy on Incomplete Fusion at E= 4-7Mev/," *Journal of Modern Physics,5 :2063-2074*, 2014

[3] Ahmad, T, Rizvi, I.A., Agarwal, A., Kumar, R., Golda, K.S. and A.K. Chaubey, *International Journal of Modern Physics E, 20, 645,* 2011

[4] Canto L, Gomes P. R. S, Don Angelo R, M. S. Hussein, "Coulomb and nuclear components of the breakup, their interference and effect on the fusion process," Phys. Rep. 424, 1,2006

[5]. Hodgson P. E, Gadioli, E, G. Erba, Introductory Nuclear Physics, Oxford University Press, (2003).

[6] Wong C.Y. Interaction barriers for light, weakly bound projectiles. *Phys. Rev. Lett. 31,766,* 1973

[7] Mukherjee S, et.al," Incomplete fusion reactions: analysis of excitation functions and recoil range distributions in 16-O+51-V," *European Physical Journal A: Hadrons and Nuclei;* Vol.12: p.199 2001

[8] International Atomic Energy Agency (IAEA)-Nuclear Data Services, Experimental Nuclear Reaction Data (EXFOR), Vienna, Australia, url: http://www-nds.iaea.org/exfor/exfor.htm

[9] Hill, D.L, J.A. Wheeler, "Nuclear Constitution and the Interpretation of Fission Phenomena," *Phys. Rev.* 89: 1102, 1953

[10] Glass, D. Mosel, "Limitation on complete fusion during heavy-ion collisions," *Phys. Rev* C10, 2620 1974.see also *Nucl. Phys*, A 237 429, 1974

[11] Otto S.R, J.P. Denier, An introduction to programming and Numerical Methods in MATLAB. *Springer-Verlag London Limited*.225 240, 2005

[12] Freitas A. S, Marques L, Zhang X.X, Luzio M. A, Guillamon P, Condori R. P, R. Lichtenthaler, "Wood-Saxon equivalent to a double folding potential," *Instituto de fisica da Universidad de Sao Paulo,* CP. 66318, 05389-970, 2015

[13] Dasgupta M. et al, Phys.Rev.C73 (034607), 2006

[14] Gomes P R S et al, "Simultaneous optical model analysis of elastic scattering, fusion and breakup for the Be^{9} + Sm^{144} system at near-barrier energies," *Phys. Rev.* C77 (2008) 054606, 2008